Published in final edited form as:
J Immunol. 2009 October 1; 183(7): 4545–4553. doi:10.4049/jimmunol.0900673.

Temporal Regulation of Ig Gene Diversification Revealed by Single-Cell Imaging[1]

Ellen C. Ordinario[2,3,‡], **Munehisa Yabuki**[2,*], **Ryan P. Larson**[*], and **Nancy Maizels**[*,‡]
[*]Department of Immunology, University of Washington School of Medicine, Seattle, WA 98195
[‡]Department of Biochemistry, University of Washington School of Medicine, Seattle, WA 98195

Abstract

Rearranged Ig V regions undergo AID-initiated diversification in sequence to produce either nontemplated or templated mutations, in the related pathways of somatic hypermutation and gene conversion. In chicken DT40 B cells, gene conversion normally predominates, producing mutations templated by adjacent pseudo-V regions; but impairment of gene conversion switches mutagenesis to a nontemplated pathway. We recently showed that the activator, E2A, functions in *cis* to promote diversification, and that G1 phase of cell cycle is the critical window for E2A action. By single-cell imaging of stable AID-YFP transfectants, we now demonstrate that AID-YFP can stably localize to the nucleus in G1 phase, but undergoes ubiquitin-dependent proteolysis later in cell cycle. By imaging of DT40 PolyLacO-λ_R cells, in which polymerized lactose operator tags the rearranged λ_R gene, we show that both the repair polymerase Polη and the multifunctional factor MRE11/RAD50/NBS1 localize to λ_R, and that λ_R/Polη colocalizations occur predominately in G1 phase, when they reflect repair of AID-initiated damage. We find no evidence of induction of γ-H2AX, the phosphorylated variant histone that is a marker of double-strand breaks, and Ig gene conversion may therefore proceed by a pathway involving templated repair at DNA nicks rather than double-strand breaks. These results lead to a model in which Ig gene conversion initiates and is completed or nearly completed in G1 phase. AID deaminates single-stranded DNA, and restriction of mutagenesis to G1 phase would contribute to protecting the genome from off-target attack by AID when DNA replication occurs in S phase.

Introduction

The V regions of actively transcribed Ig genes undergo physiologically induced and regulated sequence diversification, which expands and modulates the repertoire for antigen recognition and provides a dynamic response to infection by pathogenic microorganisms (1-5). V region diversification produces two distinct mutagenic signatures: somatic hypermutation introduces nontemplated single base changes, while gene conversion uses upstream pseudo-V (ψV) gene segments as templates for mutagenesis (2,6-11). Gene conversion is the primary source of diversity in the pre-immune antibody repertoire of chicken and other fowl. Somatic hypermutation occurs in antigen-activated human and murine B cells and also diversifies the pre-immune repertoire in other species, such as sheep (12).

[1]This work was supported by National Institutes of Health Grants R01 GM39799 and R01 GM41712 (to N.M.) and National Institutes of Health Predoctoral Training Programs T32 GM07223 and T32 AG00057 (to E.C.O.).

Address correspondence and reprint requests to Dr. Nancy Maizels, Department of Immunology, 474A HSB, University of Washington School of Medicine, Seattle, WA 98195-7650. maizels@u.washington.edu.
[2]E.C.O. and M.Y. contributed equally to this work.
[3]Current address: Life Sciences Division, Lawrence Berkeley National Laboratory, University of California, Berkeley, CA 94720

The mechanisms of somatic hypermutation and gene conversion are closely related, as first proposed over a decade ago (13). Both processes are initiated by attack of the B cell-specific enzyme, activation-induced deaminase (AID), on actively transcribed Ig genes (14-17). AID deaminates cytosine to uracil in DNA (18-21). Mutagenic repair then depends either on uracil-DNA glycosylase (UNG), which removes uracil to create an abasic (AP) site; or MutSα (MSH2/MSH6), which recognizes U·G mismatches (22). The multifunctional MRE11/RAD50/NBS1 (MRN) complex (23-25) associates with and is enriched at diversifying Ig genes, where it may promote V region gene conversion by employing its AP lyase activity to cleave at the AID-initiated AP site (26,27); by tethering DNA molecules for recombination (24); and/or by carrying out DNA resection necessary for homology-dependent repair (28). The repair polymerase, Polη, participates in both gene conversion (29,30) and somatic hypermutation (31-35), and can generate the templated mutations characteristic of normally proliferating chicken B cells. Point mutations accumulate if gene conversion is impaired by a variety of strategies, including ablation of critical factors, such as the RAD51 paralogs (RAD51B, RAD51C, RAD51D, XRCC2, and XRCC3) (36-38), or BRCA1 and BRCA2 (39,40); or deletion of (41) or repressive chromatin modifications at (42) ψV donors, probably as a result of recruitment of this and/or other low fidelity polymerases to sites of AID-initiated DNA damage.

We recently showed that activation of Ig gene diversification depends upon *cis*-interactions of the Igλ allele with the regulatory factor E2A that occur in G1 phase of cell cycle (43). Those experiments took advantage of the ability to directly image diversifying λ_R genes in single DT40 PolyLacO-λ_R B cells. These cells are derivatives of the chicken bursal lymphoma line DT40, in which polymerized lactose operator (PolyLacO) has been inserted just upstream of the rearranged and expressed λ light chain gene (42,43). By single-cell imaging, we now demonstrate that AID-YFP can stably localize in the nuclei of cells in G1 phase, but not in S phase or later stages. Colocalizations of λ_R with the polymerase Polη occur predominately in G1 phase. We find no evidence for induction of γ-H2AX, the phosphorylated variant histone that is a hallmark for DNA double-strand breaks (DSBs), at any stage of cell cycle. These results suggest that Ig gene conversion involves a DNA intermediate that carries a nick, rather than a DSB, and that gene conversion may initiate and be nearly completed in G1 phase of cell cycle.

Materials and Methods

Cell culture

DT40 and its derivative cell lines were cultured and transfected as previously described (26,43). Leptomycin B (LMB; Sigma-Aldrich) and MG132 (Z-Leu-Leu-Leu-aldehyde; Sigma-Aldrich) were added at 50 ng/ml and 50 μM, respectively, for indicated times. 5-bromo-2′-deoxyuridine (BrdU; Sigma-Aldrich) was added at 10 μM for 30 min to pulse label cells. Irradiation was carried out at 8 Gy using a ^{137}Cs irradiator. The sIgM-loss assay was conducted as described (26,38,43), and results were compared with the Mann-Whitney *U* test.

Plasmid constructs

An AID-YFP expression construct was generated by cloning an AID cDNA of DT40 into the *Bgl*II site of pEYFP-N1 (Clontech). AIDΔC, which lacks the C-terminal 16 amino acids, was generated by amplification with primers 5′-CCAGAGATCTGAGAGAGAACCCAGCTGACATG-3′ and 5′-TTAAAGATCTGGCAGAAGGATCCGTCGGAGTTTCCTGGA-3′ and similarly cloned into the *Bgl*II site of pEYFP-N1. Three phosphorylation-site mutants, AID^{T27A}, AID^{S38A} and AID^{Y184A}, were generated by QuikChange site-directed mutagenesis (Stratagene). A

Polη-GFP expression construct (44) was provided by Dr. James Cleaver (University of California, San Francisco, CA). A Ugi expression construct (45) was provided by Dr. Michael Neuberger (Medical Research Council Laboratory of Molecular Biology, Cambridge, UK).

Immunofluorescence staining and image analysis

Immunofluorescence staining was performed as previously described (43). Primary antibodies used were: anti-GFP (3E6, 1:100; Molecular Probes); anti-NBS1 (1:25; provided by Dr. Pat Concannon, University of Virginia, Charlottesville, VA; or 1:1000; affinity purified rabbit antibody raised against a peptide corresponding to the C-terminal 20 amino acids of murine NBS1); anti-γ-H2AX (JBW3C1, 1:200; Upstate; or BL178, 1:500; Bethyl Laboratories); anti-FG-containing nuclear pore proteins (Mab414, 1:5000; Covance); anti-Golgi 58K protein (58K-9, 1:1000; Sigma); anti-ubiquitin (ab8134, 1:200; Abcam); and anti-SUMO1 (21C7, 1:200; Zymed). The BrdU labeling and detection kit I (Roche) was used to detect incorporated BrdU. Alexa Fluor 488- or 594-conjugated anti-IgG (Molecular Probes) were used as secondary antibodies. DNA was stained with 4,6-diamidino-2-phenylindole (DAPI; Sigma-Aldrich).

For imaging of AID-YFP transfectants, we screened multiple independent clones and selected for imaging the two transfectant clones in which the AID-YFP signal was brightest. Results with these two clones were comparable, and detailed analysis of one clone is presented. In that clone, AID-YFP was more than 10-fold overexpressed relative to endogenous AID, as estimated by RT-PCR. Nuclear localization of AID-YFP was examined using a line profile tool of the softWoRx software (Applied Precision), and cells scored as positive if a YFP signal above background was detected throughout the nucleus. Cell cycle stage was determined by BrdU staining or estimated based on the nuclear size: G1, $r < 4\ \mu m$; G2, $r \geq 5.2\ \mu m$ (43). For experiments in which BrdU-staining was used to establish cell cycle stage, DNase treatment (Roche) was used to render DNA single-stranded and expose the newly incorporated BrdU to antibodies. This interferes minimally with the YFP signal but does not create as intense a BrdU signal as denaturation with alkali. Only cells containing five or more distinct BrdU foci were scored as S-phase cells, in order to exclude cells in other stages of cell cycle in which repair DNA synthesis was ongoing. The fraction of S phase cells as determined by BrdU staining was therefore lower than the fraction determined by propidium iodide staining and flow cytometry (36% compared to 56%).

To quantitate colocalizations in DT40 PolyLacO-λ_R and DT40 PolyLacO-λ_U derivatives, fluorescent images were acquired using the DeltaVision deconvolution microscopy system (Applied Precision) and processed and analyzed with softWoRx and Imaris (Bitplane) softwares. Fluorescence signals were sometimes partially rather than completely overlapping, which may reflect the considerable distance (~17 kb) between the PolyLacO-tag and the Vλ region, and were scored as colocalizing if the distance of fluorescent peaks was $< 0.2\ \mu m$. Significance of colocalization and cell cycle distribution were analyzed with the Pearson's χ^2 test.

UNG assay

UNG activity in nuclear extracts was assayed as described (27,45). The substrate oligonucleotide was 5′-CAGAAAGGGAAAGTATACAACAAAAAGCA<u>U</u>CTCAAGTCTTGGAGAGAACA-3′, which was 5′-end labeled using T4 polynucleotide kinase (New England BioLabs) and γ-^{32}P-ATP (PerkinElmer).

Results

Regulated localization of AID in the DT40 nucleus

We assayed subcellular localization of AID in the chicken B cell line DT40, which derives from a bursal lymphoma and carries out constitutive Ig gene diversification (10,11,46). AID carries a strong nuclear export signal (NES) which specifies export via the nuclear pore, using the CRM1-mediated pathway, and AID has been shown to localize predominantly to the cytoplasm in mammalian cells (47-51). To examine AID localization by single-cell imaging, we constructed a vector expressing chicken AID carrying a C-terminal yellow fluorescent protein tag (AID-YFP). Tagging AID at this position has been shown not to interfere with protein function (47,52). By analysis of sIgM loss rate (43) of 24 independent DT40 AID-YFP transfectants, we determined that stable expression of AID-YFP accelerated the clonal rate of Ig gene diversification 2.5-fold ($p = 0.0014$, Mann-Whitney *U* test), comparable to results obtained by others (e.g. (41,47)). We imaged AID-YFP localization by fluorescence microscopy. AID-YFP localized to the cytoplasm, forming dots or flares just outside the nucleus rather than a diffuse signal (e.g. Fig. 1A, left). Others have similarly observed that, in mammalian B cells, AID cytoplasmic signals may be threadlike (47) or concentrated in pockets on the nuclear surface (51). Using quantitation with a line profile tool of the softWoRx imaging software as the criterion for distinguishing nuclear/cytoplasmic distribution of AID, we confirmed the nuclear level of AID-YFP to be very low, indistinguishable from background (Fig. 1A, right). We further verified that cytoplasmic localization of AID is determined by the conserved C-terminal NES, as shown for AID in mammals, by demonstrating that deletion of the NES resulted in nuclear accumulation (AIDΔC-YFP; e.g. Fig. 1B, left). This was also confirmed by analysis with the line profile tool (Fig. 1B, right).

AID function is regulated in part by phosphorylation, and mutation of Ser38, a protein kinase A phosphorylation site, has been shown to affect AID function in Ig gene diversification (53-57). To test the possible role of regulatory phosphorylation in nuclear localization, we asked if localization was affected by mutation at Ser38 as well as two other phosphorylation sites, Thr27 and Tyr184. We generated stable AID^{T27A}-YFP, AID^{S38A}-YFP and AID^{Y184A}-YFP transfectants, and assayed localization of each. All localized to the cytoplasm, but AID^{S38A}-YFP also formed a few nuclear foci (Figure 1C), suggesting that regulatory phosphorylation at this site may be important for AID localization.

Cell cycle-dependence of AID nuclear localization

To test possible cell cycle-dependence of AID-YFP localization, we first attempted to identify the AID-YFP signal in fixed cells sorted following propidium iodide staining, which measures DNA content. The cell cycle distribution was similar in the AID-YFP transfectants compared to the parental DT40 cell line: 23% G1 phase, 56% S phase, 21% G2/M phase in DT40 AID-YFP transfectants; and 21% G1 phase, 55% S phase, 24% G2/M phase in the DT40 parent. However, the fixed and sorted cells had undergone significant loss of the AID-YFP signal. We therefore adopted alternative approaches to determine cell cycle phase. We have previously shown that nuclear radius corresponds closely to cell cycle stage in DT40 and its derivatives, and that nuclear radius < 4 μm provides a conservative criterion for scoring G1 phase cells (43). Cells were cultured with LMB for 30 min, fixed, imaged, and assigned to cell cycle stage based on nuclear radius. A nuclear AID-YFP signal was observed in 21% of cells ($n = 123$); and more than 80% of cells exhibiting a nuclear AID-YFP signal had nuclear radius < 4 μ, and were therefore in G1 phase (Fig. 1D, right). G1 phase cells correspond to less than 25% of the cell population, based on either cell sorting or measurements of nuclear radius. Thus there appeared to be a considerable overrepresentation of nuclear AID-YFP in G1 phase of cell cycle, and underrepresentation in later stages. In particular, these results raised the possibility that AID-YFP might be excluded from the nucleus in S phase.

To specifically assay the presence of AID-YFP in the nuclei of S phase cells, we stained with BrdU to identify cells carrying out DNA replication. Cells were cultured with LMB for 30 min, then BrdU added for an additional 30 min of culture, after which cells were fixed, DNase treated to expose incorporated BrdU to antibodies, stained with anti-BrdU antibodies and imaged (e.g. Fig. 1D, left). We scored as $BrdU^+$ only cells containing five or more nuclear BrdU foci, to exclude cells carrying out repair DNA synthesis, and tabulated $BrdU^+$ cells and cells exhibiting a nuclear AID-YFP signal (Table 1). Following culture with LMB followed by addition of BrdU, 19% of cells contained nuclear AID-YFP, but only 2.4% of cells containing nuclear AID-YFP were also $BrdU^+$ (n = 288). When LMB was included after initiation of BrdU labeling, 12% of cells contained nuclear AID-YFP, and only 1.1% of cells contained both nuclear AID-YFP and $BrdU^+$ (n = 353). Thus there is a considerable underrepresentation of AID-YFP in $BrdU^+$ cells, suggesting that AID-YFP is depleted from the nucleus when DNA replication occurs.

Levels of AID in mammalian cells are regulated by ubiquitin-dependent proteolysis, and the half-life of nuclear AID has been reported to be shorter than that of cytoplasmic AID (2.5 hr vs. 18-20 hr (52)). This suggested that proteolysis of AID may account for underrepresentation of nuclear AID-YFP in S phase cells; and predicted that culture with MG132, an inhibitor of ubiquitin-dependent proteolysis, would stabilize nuclear AID-YFP and increase the fraction of S phase cells in which it is evident. We tested this by culturing cells with MG132 and LMB for 4 hr, then analyzing AID-YFP localization as a function of cell cycle, as determined by measuring nuclear radii of individual cells (43). Nuclear AID-YFP was evident in 18% of these cells (n = 298; e.g. Fig. 1E, left), comparable to the fraction of such cells observed following culture with LMB alone (19%). However, the cell cycle distribution of cells in which a nuclear AID-YFP signal was evident was clearly shifted, so only 13% of such cells were in G1 phase, while 69% were in S phase and 18% were in G2 phase (Fig. 1E, right; n = 55). This contrasts with the distribution of cells containing nuclear AID-YFP and treated with LMB alone (Fig. 1D, right; $p < 0.001$, χ^2 test). Thus, culture with MG132 appears to stabilize nuclear AID-YFP in S phase cells, without increasing the fraction of G1 phase cells containing nuclear AID-YFP.

Culture with MG132 and LMB also promoted formation of a distinctive cytoplasmic spot of AID-YFP, which was shown to be juxtaposed to the Golgi apparatus by staining with anti-Golgi 58K antibodies (red, Fig. 1E, left). This spot is similar to the aggregates of ubiquitinated proteins, or “aggresomes” that form as consequence of inhibition of the proteasome, as documented for other proteins including the close relative of AID, APOBEC3G (58,59). To ask if these bright cytoplasmic AID-YFP spots might reflect aggregates of modified protein, we asked if they colocalized with regions stained by antibodies to ubiquitin or SUMO. There was some colocalization of the bright AID-YFP spot with regions of ubiquitin but not SUMO staining (Fig. 1F).

The results above show that while AID-YFP localizes predominately to the cytoplasm, it can be found in the nucleus in G1 phase cells. AID-YFP appears to be able to enter the nucleus throughout cell cycle, but to be destabilized by ubiquitin-dependent proteolysis outside of G1 phase.

E2A preferentially colocalizes with the rearranged λ_R allele

Many repair factors and transcription factors function in factories readily identifiable by fluorescence microscopy as distinctive foci within the nucleus, containing 50 or more protein molecules concentrated in a small nuclear volume (60). Single-cell imaging of colocalizations of foci of such factors with specific genes can provide valuable information on temporal regulation of transcription or repair. To image Ig genes in the nucleus, we have used a derivative of DT40, DT40 PolyLacO-λ_R, in which PolyLacO has been integrated by homologous gene targeting to the ψVλ array just upstream of the rearranged and expressed λ_R gene (42,43). In DT40 PolyLacO-λ_R cells, the PolyLacO tag enables the diversifying λ_R gene to be imaged directly in cells expressing green or red fluorescent proteins fused to lactose repressor (GFP-LacI or RFP-LacI), but does not alter proliferation, cell cycle distribution, the clonal rate of Ig gene conversion or local chromatin structure (42,43). Colocalizations of factors with the tagged gene can readily be quantitated in these cells by fluorescence microscopy. However, the confined nuclear space means that there will be inevitable background contributed by apparent overlap of the tagged gene and foci of transcriptional or regulatory factors. We have previously shown that the regulatory factor E2A colocalizes with the rearranged λ_R gene, and that this colocalization correlates with the *cis*-interaction essential to promote Ig gene diversification (43). In addition, by chromatin immunoprecipitation (ChIP) analysis we have shown that E2A specifically associates with the rearranged λ_R allele in DT40 cells, exhibiting an 18-fold enrichment at that allele relative to the unrearranged λ_U allele (43). Those results enabled us to ask if E2A preferentially colocalizes with the rearranged λ_R allele, as predicted by ChIP, and at the same time determine the background level of colocalizations evident as analyzed by fluorescence microscopy. To do this, we assayed colocalizations of E2A with the unrearranged λ_U light chain allele, in the DT40 PolyLacO-λ_U cell line. In that cell line, the PolyLacO tag is integrated in the ψVλ array upstream of the unrearranged and unexpressed λ_U allele (Fig. 2A). In DT40 PolyLacO-λ_U cells, proliferation (Fig. 2B), cell cycle distribution (Fig. 2C) and the clonal rates of Ig gene diversification (Fig. 2D) were comparable to the DT40 parental line, and to the DT40 PolyLacO-λ_R cells. However, while λ_R/E2A colocalizations were evident in 26% of DT40 PolyLacO-λ_R cells (n = 227) in asynchronous culture (43), λ_U/E2A colocalizations were evident in only 6.3% (n = 191) of DT40 PolyLacO-λ_U cells (Fig. 2E; $p < 0.0001$, χ^2 test). Thus, quantitation of colocalization can provide very useful information on function of a factor at a gene.

λ_R/Polη colocalizations occur preferentially in G1 phase

The repair DNA polymerase, Polη, participates not only in Ig gene diversification but also in repair of UV damage and has been shown to form repair foci after UV irradiation (44). To establish when in cell cycle repair of AID-initiated DNA damage occurs, we therefore assayed temporal regulation of localization of the repair factor Polη to λ_R in DT40 PolyLacO-λ_R cells, in which PolyLacO tags the rearranged and expressed λ_R gene (Fig. 3A). To ensure specificity in imaging Polη, we stably transfected DT40 PolyLacO-λ_R RFP-LacI cells with a Polη-GFP expression construct and stained with antibodies to the GFP tag. λ_R/Polη-GFP colocalizations were imaged by fluorescence microscopy, and cells containing colocalized foci were scored. Cell cycle profiling showed that in these transfectants, 27% of cells were in G1 phase, 56% in S phase, and 17% in G2 phase. λ_R/Polη-GFP colocalizations were observed in 11% of DT40 PolyLacO-λ_R RFP-LacI Polη-GFP cells in asynchronous cultures (n = 1,013; e.g. Fig. 3B, left). Analysis of cell cycle distribution of λ_R/Polη-GFP colocalizations showed that 39% occurred in G1 phase, 56% in S phase, and 5% in G2 phase (Fig. 3B, right). The excess of λ_R/Polη-GFP colocalizations in G1 phase and the dearth of colocalizations in G2 phase were statistically significant (p = 0.0010, χ^2 test). Similarly, we previously documented a significant excess of λ_R/E2A colocalizations in G1 phase (43).

Localization of MRN to λ_R is evident throughout cell cycle

To ask whether MRN localizations at λ_R exhibit cell cycle dependence, we imaged λ_R/NBS1 colocalizations, by staining DT40 PolyLacO-λ_R GFP-LacI cells with anti-NBS1 antibodies. λ_R/NBS1 colocalizations were evident in 17% of cells in asynchronous culture (n = 232; e.g.

Fig. 3C, left). Analysis of cell cycle distribution of λ_R/NBS1 colocalizations showed that 28% occurred in G1 phase, 48% in S phase, and 24% in G2 phase (Fig. 3C, right). This did not different significantly from the cell cycle distribution of these cells (G1, 27%; S, 56%; G2/M, 17%; $p = 0.13$, χ^2 test).

DT40 cells do not contain γ-H2AX foci, diagnostic of DSBs

Foci of the phosphorylated variant histone, γ-H2AX, are hallmarks of DSBs (61-63). We therefore stained DT40 cells with antibodies to γ-H2AX to determine whether DSBs are an intermediate in Ig gene conversion, but this produced only very faint signals in DT40 PolyLacO-λ_R GFP-LacI cells, and λ_R/γ-H2AX colocalizations were not evident (not shown). We then quantitated γ-H2AX foci in the DT40 parental cell line, to ensure that the strong signal from the tagged λ_R gene would not interfere with the weak γ-H2AX signal. We found that most cells in asynchronous DT40 cultures contained no γ-H2AX foci (88%, $n = 410$; e.g. Fig. 3D, above left), but a small fraction of cells contained 1-3 small, faint, and punctate foci (12%; e.g. Fig. 3D, above left), similar to those observed in other cell lines proliferating under normal conditions (62,64). Analysis of cells sorted by cell cycle stage prior to staining showed that faint γ-H2AX foci were present in 2.3% of G1 phase, 9.0% of S phase, and 7.7% of G2 phase cells ($n > 300$ in each case; Fig. 3D above right). In contrast, NBS1 foci were present in 37% of G1 phase, 54% of S phase, and 43% of G2 phase cells (Fig. 3D, above right), but there was no evidence of colocalization of γ-H2AX and NBS1. Following treatment with ionizing radiation (IR), which induces DSBs, brightly staining γ-H2AX foci were induced and colocalized with NBS1, as has been reported for many other cell types: 3 or more γ-H2AX/NBS1 colocalized foci were evident in 38% of cells ($n = 312$; e.g. Fig. 3D, lower). Thus, bright γ-H2AX foci can form in DT40 cells, but γ-H2AX foci do not characterize cells carrying out gene conversion. This suggests that if a DSB is formed in the course of gene conversion, it is present only very transiently, or does not associate with γ-H2AX in the course of repair.

G1 phase λ_R/Polη colocalizations are UNG-dependent

G1 phase is the window in which AID can stably localize to the nucleus (Fig. 1) and in which E2A activates diversification at the Ig genes (43). This suggested that λ_R/Polη-GFP colocalizations in G1 phase may reflect repair synthesis at the diversifying V region. To test this, we examined the effect of uracil-DNA glycosylase inhibitor (Ugi) expression on λ_R/Polη-GFP colocalizations. Ugi inhibits UNG, and expression of Ugi in DT40 B cells inhibits Ig gene conversion (65). We generated stable DT40 PolyLacO-λ_R RFP-LacI Polη-GFP Ugi transfectants, and verified inhibition of UNG activity upon Ugi expression by assaying deglycosylation of a uracil-containing, 5′-end-labeled synthetic oligonucleotide by nuclear extracts from the parental cell line and the Ugi-expressing derivative (Fig. 4A). Single-cell imaging showed that λ_R/Polη-GFP colocalizations were evident in 5.4% of asynchronous DT40 PolyLacO-λ_R RFP-LacI Polη-GFP Ugi cells ($n = 298$), compared with 11% of parental DT40 PolyLacO-λ_R RFP-LacI Polη-GFP cells ($p = 0.0035$, χ^2 test). In DT40 PolyLacO-λ_R RFP-LacI Polη-GFP Ugi cells, 19% of colocalizations occurred in G1 phase (Fig. 4B; $p < 0.001$ vs. 39% in the parental line, χ^2 test), 75% in S phase, and 6.3% in G2 phase.

To better gauge the effect of Ugi, λ_R/Polη-GFP colocalizations in each phase of cell cycle were graphed as a fraction of the entire cell population. This showed that, in Ugi-expressing cells, the percentage of G1 phase cells containing λ_R/Polη-GFP colocalizations was reduced from 4.5% to 1.0%, or 4.4-fold (Fig. 4C; $p = 0.011$, χ^2 test). In contrast, the percentage of S phase cells containing λ_R/Polη-GFP colocalizations was reduced from 6.3% to 4.0% ($p = 0.20$, χ^2 test); and the percentage of G2 phase cells containing λ_R/Polη-GFP colocalizations was reduced from 0.6% to 0.3% ($p = 0.63$, χ^2 test). Thus, only in G1 phase did Ugi expression have a significant effect on the fraction of cells containing λ_R/Polη-GFP colocalizations. While we cannot eliminate the possibility that Ugi expression has subtle effects on DNA metabolism throughout cell cycle, the simplest interpretation of these results is that the G1 phase-specific colocalizations reflect repair initiated by AID and UNG. This suggests that G1 phase is the window in which much of the repair synthesis that is induced in response to AID-initiated DNA damage occurs.

Discussion

Regulation of Ig gene diversification in the course of cell cycle

Using single-cell imaging to analyze temporal regulation of Ig gene conversion, we have found that two key factors act primarily in G1 phase of cell cycle. AID-YFP stably localizes to the nucleus in G1 phase, but not other phases of cell cycle; and Polη localizes to the Igλ locus predominately in G1 phase. AID initiates gene conversion, and repair synthesis by Polη is a late step in the mutagenic pathway. These results complement earlier evidence that G1 phase is key to activation of Ig gene diversification by E2A (43), and raise the possibility that gene conversion may initiate and be nearly completed in G1 phase, prior to DNA replication in S phase.

AID preferentially deaminates single-stranded DNA (19-21,66). The transient DNA denaturation essential for replication would therefore be predicted to create a target for AID. Restricting AID attack to G1 phase would therefore protect the replicating genome from AID-initiated mutagenesis or other forms of genomic instability, such as translocation. In addition, mutations created in G1 phase could be fixed in the subsequent S phase (Fig. 5) and thereby protected from post-replicative repair which would have an adverse effect on mutagenesis essential to the immune response.

Spatiotemporal regulation of AID localization to the nucleus

To analyze regulation of AID, we generated a snapshot of AID-YFP subcellular localization by treating cells briefly with LMB, which inhibits CRM1-dependent nuclear export, and then distinguishing S phase cells by nuclear size and/or BrdU staining. This analysis showed that AID-YFP was present in the nucleus in early stages of cell cycle, but absent from the nucleus in S and later stages, when DNA replication occurs. Inhibition of ubiquitin-dependent proteolysis altered cell cycle dependence of AID-YFP localization, increasing the fraction of S phase cells in which AID-YFP was observed. Like its close relative, APOBEC3G (59), AID-YFP accumulated in cytoplasmic aggresomes upon inhibition of proteasomal degradation. These experiments analyzed localization of tagged fluorescent protein in stable AID-YFP transfectants, so we cannot preclude the possibility that some of the observed effects were due to overexpression of AID. Nonetheless, this evidence for nuclear instability of AID-YFP in chicken B cells is consistent with analysis of mammalian cells, which demonstrated that the half-life of nuclear AID is eight-fold below that of cytoplasmic AID (52). These results therefore suggest that regulatory proteolysis prevents accumulation of AID-YFP in the nucleus at stages of cell cycle later than G1 phase.

Distinct temporal regulation of colocalizations of λ_R with Polη and the MRN complex

Single-cell imaging showed that both the repair polymerase Polη and the MRN complex localize to the diversifying λ_R allele in DT40 B cells. The visual evidence provided by analysis of colocalizations complements genetic and biochemical evidence for function of Polη and MRN in Ig gene conversion (26-30). Imaging further suggests that localizations of Polη and MRN to the Ig genes are under distinct temporal regulation. Colocalizations of λ_R with Polη-GFP occurred predominately in G1 phase; and expression of Ugi, which inhibits UNG activity and thereby mutagenic repair downstream of deamination of cytosine to uracil, diminished colocalizations in G1 phase over 4-fold, but had relatively modest effect on colocalizations in other stages of cell cycle.

In contrast, colocalizations of λ_R with NBS1 occurred throughout cell cycle. This may reflect the multiple roles played by the multifunctional MRN complex. Gene conversion depends on factors that promote homology-dependent repair, which occurs primarily in S and G2 phases. Gene conversion may be prolonged into S phase to take advantage of elevated levels of those factors in that phase of cell cycle. If so, then MRN may function differently at the V region in each stage of cell cycle, using its AP lyase to initiate diversification in G1 phase and then resecting the DNA or tethering recipient and donor later in cell cycle. This is distinct from MRN function in switching B cells, where nonhomologous end-joining (NHEJ) promotes DSB repair, and NBS1 colocalizes with the IgH locus predominately in G1 phase (67), when the NHEJ pathway is most active (63,68-71).

DNA intermediates for Ig gene conversion may carry nicks rather than DSBs

In principle, gene conversion can involve a DNA intermediate carrying either a DNA DSB or nick. In one example studied in considerable mechanistic detail, mating type switching in the yeast, *S. cerevisiae*, is initiated by a DNA DSB (72). However, DNA nicks have also been shown to be effective in initiating recombinational repair (73,74). We assayed for DSBs by staining DT40 cells for foci of γ-H2AX, diagnostic of DNA DSBs (61-63). We found no evidence of such foci in normally proliferating DT40 cells, although bright γ-H2AX foci were inducible by IR. This suggests that gene conversion at the Ig loci does not involve DSBs; or if DSBs do form, they are present only very transiently.

At the diversifying Ig loci, AID, UNG and MRN act sequentially to generate a nick, in a series of steps common to gene conversion and somatic hypermutation (Fig. 5). If a nick rather than a DSB initiates recombinational repair, then this suggests a model in which a nick generated in G1 phase after successive action of AID, UNG and MRN would be repaired in G1 phase by Polη, and by other recombination factors in later cell cycle stages (Fig. 5). This model does not postulate involvement of DSBs or γ-H2AX.

Two groups have shown that deficiencies in NHEJ increase the rates of Ig gene conversion (75,76). This has been interpreted as evidence that gene conversion depends on DSBs, based on the view that DSBs not repaired by NHEJ would then be intermediates for gene conversion. However, products of V region gene conversion rarely carry the short deletions typical of NHEJ, making it unlikely that a significant fraction enter this pathway. The absence for evidence of γ-H2AX induction in DT40 cells suggests that impaired NHEJ may not simply increase available substrates, but have other effects on Ig gene conversion. For example, impaired NHEJ may result in activation of factors that promote homology-dependent repair, and thus increase the rates of gene conversion.

Gene conversion and somatic hypermutation are closely related

γ-H2AX is not necessary for somatic hypermutation, as mice deficient in γ-H2AX exhibit normal levels of somatic hypermutation (77). In contrast, γ-H2AX is required for Ig class switch recombination, a process of regulated DNA deletion which depends upon the NHEJ pathway and involves the formation and rejoining of DNA DSBs; and γ-H2AX is evident in distinct foci in B cells carrying out class switch recombination (67). The apparent lack of participation of γ-H2AX in Ig gene conversion (see above) and somatic hypermutation (77) reinforces the mechanistic relationship between these two processes. Both can result from templated or nontemplated mutagenesis at a DNA nick (Fig. 5). In gene conversion, strand transfer occurs to permit templated mutagenesis; while the error-prone polymerases that promote somatic hypermutation can extend directly from a DNA nick. The RAD51 paralogs promote strand transfer, and deficiencies in these factors alters the outcome of repair at the chicken Ig loci, so that hypermutation occurs rather than gene conversion (36-40), providing further support for the model that gene conversion and somatic hypermutation proceed via the same DNA intermediate.

Acknowledgments

We thank Dr. Erik Larson for help with UNG assays; Monica Fujii for assistance in preliminary experiments; Greg Martin (Keck Imaging Center, University of Washington) for help with fluorescence microscopy; and Drs. Yansong Gu, Brian Kennedy, David Morris, Dennis Willerford and all members of the Maizels laboratory for discussions.

Abbreviations used in this paper

AID	activation-induced cytidine deaminase
AP	abasic
BrdU	5-bromo-2′-deoxyuridine
DAPI	4,6-diamidino-2-phenylindole
DSB	double-strand break
GFP	green fluorescent protein
Ig	immunoglobulin
IR	ionizing radiation
LacI	lactose repressor
LMB	leptomycin B
MRN	MRE11/RAD50/NBS1
NES	nuclear export signal
NHEJ	nonhomologous end-joining
PolyLacO	polymerized lactose operator
r	nuclear radius
RFP	red fluorescent protein
SSB	single-strand break
Ugi	uracil-DNA glycosylase inhibitor
UNG	uracil-DNA glycosylase
UV	ultraviolet
V	variable
YFP	yellow fluorescent protein

References

1. Li Z, Woo CJ, Iglesias-Ussel MD, Ronai D, Scharff MD. The generation of antibody diversity through somatic hypermutation and class switch recombination. Genes Dev 2004;18:1–11. [PubMed: 14724175]
2. Maizels N. Immunoglobulin gene diversification. Annu Rev Genet 2005;39:23–46. [PubMed: 16285851]

3. Longerich S, Basu U, Alt F, Storb U. AID in somatic hypermutation and class switch recombination. Curr Opin Immunol 2006;18:164–174. [PubMed: 16464563]
4. Martomo SA, Gearhart PJ. Somatic hypermutation: subverted DNA repair. Curr Opin Immunol 2006;18:243–248. [PubMed: 16616477]
5. Di Noia JM, Neuberger MS. Molecular mechanisms of antibody somatic hypermutation. Annu Rev Biochem 2007;76:1–22. [PubMed: 17328676]
6. Reynaud CA, Anquez V, Grimal H, Weill JC. A hyperconversion mechanism generates the chicken light chain preimmune repertoire. Cell 1987;48:379–388. [PubMed: 3100050]
7. Thompson CB, Neiman PE. Somatic diversification of the chicken immunoglobulin light chain gene is limited to the rearranged variable gene segment. Cell 1987;48:369–378. [PubMed: 3100049]
8. McCormack WT, Thompson CB. Chicken IgL variable region gene conversions display pseudogene donor preference and 5′ to 3′ polarity. Genes Dev 1990;4:548–558. [PubMed: 2113879]
9. Sayegh CE, Demaries SL, Pike KA, Friedman JE, Ratcliffe MJ. The chicken B-cell receptor complex and its role in avian B-cell development. Immunol Rev 2000;175:187–200. [PubMed: 10933603]
10. Arakawa H, Buerstedde JM. Immunoglobulin gene conversion: insights from bursal B cells and the DT40 cell line. Dev Dyn 2004;229:458–464. [PubMed: 14991701]
11. Sale JE. Immunoglobulin diversification in DT40: a model for vertebrate DNA damage tolerance. DNA Repair (Amst) 2004;3:693–702. [PubMed: 15177178]
12. Reynaud CA, Garcia C, Hein WR, Weill JC. Hypermutation generating the sheep immunoglobulin repertoire is an antigen-independent process. Cell 1995;80:115–125. [PubMed: 7813007]
13. Maizels N. Somatic hypermutation: how many mechanisms diversify V region sequences? Cell 1995;83:9–12. [PubMed: 7553877]
14. Muramatsu M, Kinoshita K, Fagarasan S, Yamada S, Shinkai Y, Honjo T. Class switch recombination and hypermutation require activation-induced cytidine deaminase (AID), a potential RNA editing enzyme. Cell 2000;102:553–563. [PubMed: 11007474]
15. Revy P, Muto T, Levy Y, Geissmann F, Plebani A, Sanal O, Catalan N, Forveille M, Dufourcq-Labelouse R, Gennery A, Tezcan I, Ersoy F, Kayserili H, Ugazio AG, Brousse N, Muramatsu M, Notarangelo LD, Kinoshita K, Honjo T, Fischer A, Durandy A. Activation-induced cytidine deaminase (AID) deficiency causes the autosomal recessive form of the Hyper-IgM syndrome (HIGM2). Cell 2000;102:565–575. [PubMed: 11007475]
16. Arakawa H, Hauschild J, Buerstedde JM. Requirement of the activation-induced deaminase (AID) gene for immunoglobulin gene conversion. Science 2002;295:1301–1306. [PubMed: 11847344]
17. Harris RS, Sale JE, Petersen-Mahrt SK, Neuberger MS. AID is essential for immunoglobulin V gene conversion in a cultured B cell line. Curr Biol 2002;12:435–438. [PubMed: 11882297]
18. Petersen-Mahrt SK, Harris RS, Neuberger MS. AID mutates E. coli suggesting a DNA deamination mechanism for antibody diversification. Nature 2002;418:99–103. [PubMed: 12097915]
19. Bransteitter R, Pham P, Scharff MD, Goodman MF. Activation-induced cytidine deaminase deaminates deoxycytidine on single-stranded DNA but requires the action of RNase. Proc Natl Acad Sci U S A 2003;100:4102–4107. [PubMed: 12651944]
20. Chaudhuri J, Tian M, Khuong C, Chua K, Pinaud E, Alt FW. Transcription-targeted DNA deamination by the AID antibody diversification enzyme. Nature 2003;422:726–730. [PubMed: 12692563]
21. Ramiro AR, Stavropoulos P, Jankovic M, Nussenzweig MC. Transcription enhances AID-mediated cytidine deamination by exposing single-stranded DNA on the nontemplate strand. Nat Immunol 2003;4:452–456. [PubMed: 12692548]
22. Rada C, Di Noia JM, Neuberger MS. Mismatch recognition and uracil excision provide complementary paths to both Ig switching and the A/T-focused phase of somatic mutation. Mol Cell 2004;16:163–171. [PubMed: 15494304]
23. Paull TT, Lee JH. The Mre11/Rad50/Nbs1 complex and its role as a DNA double-strand break sensor for ATM. Cell Cycle 2005;4:737–740. [PubMed: 15908798]

24. Williams RS, Williams JS, Tainer JA. Mre11-Rad50-Nbs1 is a keystone complex connecting DNA repair machinery, double-strand break signaling, and the chromatin template. Biochem Cell Biol 2007;85:509–520. [PubMed: 17713585]

25. Stracker TH, Petrini JH. Working together and apart: the twisted relationship of the Mre11 complex and Chk2 in apoptosis and tumor suppression. Cell Cycle 2008;7:3618–3621. [PubMed: 19029802]

26. Yabuki M, Fujii MM, Maizels N. The MRE11-RAD50-NBS1 complex accelerates somatic hypermutation and gene conversion of immunoglobulin variable regions. Nat Immunol 2005;6:730–736. [PubMed: 15937485]

27. Larson ED, Cummings WJ, Bednarski DW, Maizels N. MRE11/RAD50 cleaves DNA in the AID/UNG-dependent pathway of immunoglobulin gene diversification. Mol Cell 2005;20:367–375. [PubMed: 16285919]

28. Nakahara M, Sonoda E, Nojima K, Sale JE, Takenaka K, Kikuchi K, Taniguchi Y, Nakamura K, Sumitomo Y, Bree RT, Lowndes NF, Takeda S. Genetic evidence for single-strand lesions initiating Nbs1-dependent homologous recombination in diversification of Ig v in chicken B lymphocytes. PLoS Genet 2009;5:e1000356. [PubMed: 19180185]

29. Kawamoto T, Araki K, Sonoda E, Yamashita YM, Harada K, Kikuchi K, Masutani C, Hanaoka F, Nozaki K, Hashimoto N, Takeda S. Dual roles for DNA polymerase eta in homologous DNA recombination and translesion DNA synthesis. Mol Cell 2005;20:793–799. [PubMed: 16337602]

30. McIlwraith MJ, Vaisman A, Liu Y, Fanning E, Woodgate R, West SC. Human DNA polymerase eta promotes DNA synthesis from strand invasion intermediates of homologous recombination. Mol Cell 2005;20:783–792. [PubMed: 16337601]

31. Rogozin IB, Pavlov YI, Bebenek K, Matsuda T, Kunkel TA. Somatic mutation hotspots correlate with DNA polymerase eta error spectrum. Nat Immunol 2001;2:530–536. [PubMed: 11376340]

32. Zeng X, Winter DB, Kasmer C, Kraemer KH, Lehmann AR, Gearhart PJ. DNA polymerase eta is an A-T mutator in somatic hypermutation of immunoglobulin variable genes. Nat Immunol 2001;2:537–541. [PubMed: 11376341]

33. Delbos F, De Smet A, Faili A, Aoufouchi S, Weill JC, Reynaud CA. Contribution of DNA polymerase eta to immunoglobulin gene hypermutation in the mouse. J Exp Med 2005;201:1191–1196. [PubMed: 15824086]

34. Martomo SA, Yang WW, Wersto RP, Ohkumo T, Kondo Y, Yokoi M, Masutani C, Hanaoka F, Gearhart PJ. Different mutation signatures in DNA polymerase eta- and MSH6-deficient mice suggest separate roles in antibody diversification. Proc Natl Acad Sci U S A 2005;102:8656–8661. [PubMed: 15939880]

35. Delbos F, Aoufouchi S, Faili A, Weill JC, Reynaud CA. DNA polymerase eta is the sole contributor of A/T modifications during immunoglobulin gene hypermutation in the mouse. J Exp Med 2007;204:17–23. [PubMed: 17190840]

36. Takata M, Sasaki MS, Sonoda E, Fukushima T, Morrison C, Albala JS, Swagemakers SM, Kanaar R, Thompson LH, Takeda S. The Rad51 paralog Rad51B promotes homologous recombinational repair. Mol Cell Biol 2000;20:6476–6482. [PubMed: 10938124]

37. Takata M, Sasaki MS, Tachiiri S, Fukushima T, Sonoda E, Schild D, Thompson LH, Takeda S. Chromosome instability and defective recombinational repair in knockout mutants of the five Rad51 paralogs. Mol Cell Biol 2001;21:2858–2866. [PubMed: 11283264]

38. Sale JE, Calandrini DM, Takata M, Takeda S, Neuberger MS. Ablation of XRCC2/3 transforms immunoglobulin V gene conversion into somatic hypermutation. Nature 2001;412:921–926. [PubMed: 11528482]

39. Hatanaka A, Yamazoe M, Sale JE, Takata M, Yamamoto K, Kitao H, Sonoda E, Kikuchi K, Yonetani Y, Takeda S. Similar effects of Brca2 truncation and Rad51 paralog deficiency on immunoglobulin V gene diversification in DT40 cells support an early role for Rad51 paralogs in homologous recombination. Mol Cell Biol 2005;25:1124–1134. [PubMed: 15657438]

40. Longerich S, Orelli BJ, Martin RW, Bishop DK, Storb U. Brca1 in immunoglobulin gene conversion and somatic hypermutation. DNA Repair (Amst) 2008;7:253–266. [PubMed: 18036997]

41. Arakawa H, Saribasak H, Buerstedde JM. Activation-induced cytidine deaminase initiates immunoglobulin gene conversion and hypermutation by a common intermediate. PLoS Biol 2004;2:e179. [PubMed: 15252444]

42. Cummings WJ, Yabuki M, Ordinario EC, Bednarski DW, Quay S, Maizels N. Chromatin structure regulates gene conversion. PLoS Biol 2007;5:e246. [PubMed: 17880262]

43. Yabuki M, Ordinario EC, Cummings WJ, Fujii MM, Maizels N. E2A acts in cis in G1 phase of cell cycle to promote Ig gene diversification. J Immunol 2009;182:408–415. [PubMed: 19109172]

44. Thakur M, Wernick M, Collins C, Limoli CL, Crowley E, Cleaver JE. DNA polymerase eta undergoes alternative splicing, protects against UV sensitivity and apoptosis, and suppresses Mre11-dependent recombination. Genes Chromosomes Cancer 2001;32:222–235. [PubMed: 11579462]

45. Di Noia J, Neuberger MS. Altering the pathway of immunoglobulin hypermutation by inhibiting uracil-DNA glycosylase. Nature 2002;419:43–48. [PubMed: 12214226]

46. Yamazoe M, Sonoda E, Hochegger H, Takeda S. Reverse genetic studies of the DNA damage response in the chicken B lymphocyte line DT40. DNA Repair (Amst) 2004;3:1175–1185. [PubMed: 15279806]

47. Rada C, Jarvis JM, Milstein C. AID-GFP chimeric protein increases hypermutation of Ig genes with no evidence of nuclear localization. Proc Natl Acad Sci U S A 2002;99:7003–7008. [PubMed: 12011459]

48. Ito S, Nagaoka H, Shinkura R, Begum N, Muramatsu M, Nakata M, Honjo T. Activation-induced cytidine deaminase shuttles between nucleus and cytoplasm like apolipoprotein B mRNA editing catalytic polypeptide 1. Proc Natl Acad Sci U S A 2004;101:1975–1980. [PubMed: 14769937]

49. McBride KM, Barreto V, Ramiro AR, Stavropoulos P, Nussenzweig MC. Somatic hypermutation is limited by CRM1-dependent nuclear export of activation-induced deaminase. J Exp Med 2004;199:1235–1244. [PubMed: 15117971]

50. Brar SS, Watson M, Diaz M. Activation-induced cytosine deaminase (AID) is actively exported out of the nucleus but retained by the induction of DNA breaks. J Biol Chem 2004;279:26395–26401. [PubMed: 15087440]

51. Yang G, Obiakor H, Sinha RK, Newman BA, Hood BL, Conrads TP, Veenstra TD, Mage RG. Activation-induced deaminase cloning, localization, and protein extraction from young VH-mutant rabbit appendix. Proc Natl Acad Sci U S A 2005;102:17083–17088. [PubMed: 16280388]

52. Aoufouchi S, Faili A, Zober C, D'Orlando O, Weller S, Weill JC, Reynaud CA. Proteasomal degradation restricts the nuclear lifespan of AID. J Exp Med 2008;205:1357–1368. [PubMed: 18474627]

53. Basu U, Chaudhuri J, Alpert C, Dutt S, Ranganath S, Li G, Schrum JP, Manis JP, Alt FW. The AID antibody diversification enzyme is regulated by protein kinase A phosphorylation. Nature 2005;438:508–511. [PubMed: 16251902]

54. Pasqualucci L, Kitaura Y, Gu H, Dalla-Favera R. PKA-mediated phosphorylation regulates the function of activation-induced deaminase (AID) in B cells. Proc Natl Acad Sci U S A 2006;103:395–400. [PubMed: 16387847]

55. McBride KM, Gazumyan A, Woo EM, Barreto VM, Robbiani DF, Chait BT, Nussenzweig MC. Regulation of hypermutation by activation-induced cytidine deaminase phosphorylation. Proc Natl Acad Sci U S A 2006;103:8798–8803. [PubMed: 16723391]

56. Chatterji M, Unniraman S, McBride KM, Schatz DG. Role of activation-induced deaminase protein kinase A phosphorylation sites in Ig gene conversion and somatic hypermutation. J Immunol 2007;179:5274–5280. [PubMed: 17911613]

57. Cheng HL, Vuong BQ, Basu U, Franklin A, Schwer B, Astarita J, Phan RT, Datta A, Manis J, Alt FW, Chaudhuri J. Integrity of the AID serine-38 phosphorylation site is critical for class switch recombination and somatic hypermutation in mice. Proc Natl Acad Sci U S A 2009;106:2717–2722. [PubMed: 19196992]

58. Johnston JA, Ward CL, Kopito RR. Aggresomes: a cellular response to misfolded proteins. J Cell Biol 1998;143:1883–1898. [PubMed: 9864362]

59. Wichroski MJ, Ichiyama K, Rana TM. Analysis of HIV-1 viral infectivity factor-mediated proteasome-dependent depletion of APOBEC3G: correlating function and subcellular localization. J Biol Chem 2005;280:8387–8396. [PubMed: 15537645]
60. Haaf T, Hayman DL, Schmid M. Quantitative determination of rDNA transcription units in vertebrate cells. Exp Cell Res 1991;193:78–86. [PubMed: 1995304]
61. Rogakou EP, Pilch DR, Orr AH, Ivanova VS, Bonner WM. DNA double-stranded breaks induce histone H2AX phosphorylation on serine 139. J Biol Chem 1998;273:5858–5868. [PubMed: 9488723]
62. Paull TT, Rogakou EP, Yamazaki V, Kirchgessner CU, Gellert M, Bonner WM. A critical role for histone H2AX in recruitment of repair factors to nuclear foci after DNA damage. Curr Biol 2000;10:886–895. [PubMed: 10959836]
63. Rodrigue A, Lafrance M, Gauthier MC, McDonald D, Hendzel M, West SC, Jasin M, Masson JY. Interplay between human DNA repair proteins at a unique double-strand break in vivo. EMBO J 2006;25:222–231. [PubMed: 16395335]
64. Balajee AS, Geard CR. Replication protein A and gamma-H2AX foci assembly is triggered by cellular response to DNA double-strand breaks. Exp Cell Res 2004;300:320–334. [PubMed: 15474997]
65. Di Noia JM, Neuberger MS. Immunoglobulin gene conversion in chicken DT40 cells largely proceeds through an abasic site intermediate generated by excision of the uracil produced by AID-mediated deoxycytidine deamination. Eur J Immunol 2004;34:504–508. [PubMed: 14768055]
66. Dickerson SK, Market E, Besmer E, Papavasiliou FN. AID mediates hypermutation by deaminating single stranded DNA. J Exp Med 2003;197:1291–1296. [PubMed: 12756266]
67. Petersen S, Casellas R, Reina-San-Martin B, Chen HT, Difilippantonio MJ, Wilson PC, Hanitsch L, Celeste A, Muramatsu M, Pilch DR, Redon C, Ried T, Bonner WM, Honjo T, Nussenzweig MC, Nussenzweig A. AID is required to initiate Nbs1/gamma-H2AX focus formation and mutations at sites of class switching. Nature 2001;414:660–665. [PubMed: 11740565]
68. Takata M, Sasaki MS, Sonoda E, Morrison C, Hashimoto M, Utsumi H, Yamaguchi-Iwai Y, Shinohara A, Takeda S. Homologous recombination and non-homologous end-joining pathways of DNA double-strand break repair have overlapping roles in the maintenance of chromosomal integrity in vertebrate cells. EMBO J 1998;17:5497–5508. [PubMed: 9736627]
69. Ferreira MG, Cooper JP. Two modes of DNA double-strand break repair are reciprocally regulated through the fission yeast cell cycle. Genes Dev 2004;18:2249–2254. [PubMed: 15371339]
70. Ira G, Pellicioli A, Balijja A, Wang X, Fiorani S, Carotenuto W, Liberi G, Bressan D, Wan L, Hollingsworth NM, Haber JE, Foiani M. DNA end resection, homologous recombination and DNA damage checkpoint activation require CDK1. Nature 2004;431:1011–1017. [PubMed: 15496928]
71. Aylon Y, Liefshitz B, Kupiec M. The CDK regulates repair of double-strand breaks by homologous recombination during the cell cycle. EMBO J 2004;23:4868–4875. [PubMed: 15549137]
72. Paques F, Haber JE. Multiple pathways of recombination induced by double-strand breaks in Saccharomyces cerevisiae. Microbiol Mol Biol Rev 1999;63:349–404. [PubMed: 10357855]
73. Lee GS, Neiditch MB, Salus SS, Roth DB. RAG proteins shepherd double-strand breaks to a specific pathway, suppressing error-prone repair, but RAG nicking initiates homologous recombination. Cell 2004;117:171–184. [PubMed: 15084256]
74. McConnell Smith A, Takeuchi R, Pellenz S, Davis L, Maizels N, Monnat RJ Jr. Stoddard BL. Generation of a nicking enzyme that stimulates site-specific gene conversion from the I-AniI LAGLIDADG homing endonuclease. Proc Natl Acad Sci U S A 2009;106:5099–5104. [PubMed: 19276110]
75. Tang ES, Martin A. NHEJ-deficient DT40 cells have increased levels of immunoglobulin gene conversion: evidence for a double strand break intermediate. Nucleic Acids Res 2006;34:6345–6351. [PubMed: 17142237]
76. Cook AJ, Raftery JM, Lau KK, Jessup A, Harris RS, Takeda S, Jolly CJ. DNA-Dependent Protein Kinase Inhibits AID-Induced Antibody Gene Conversion. PLoS Biol 2007;5:e80. [PubMed: 17355182]

77. Reina-San-Martin B, Difilippantonio S, Hanitsch L, Masilamani RF, Nussenzweig A, Nussenzweig MC. H2AX is required for recombination between immunoglobulin switch regions but not for intra-switch region recombination or somatic hypermutation. J Exp Med 2003;197:1767–1778. [PubMed: 12810694]

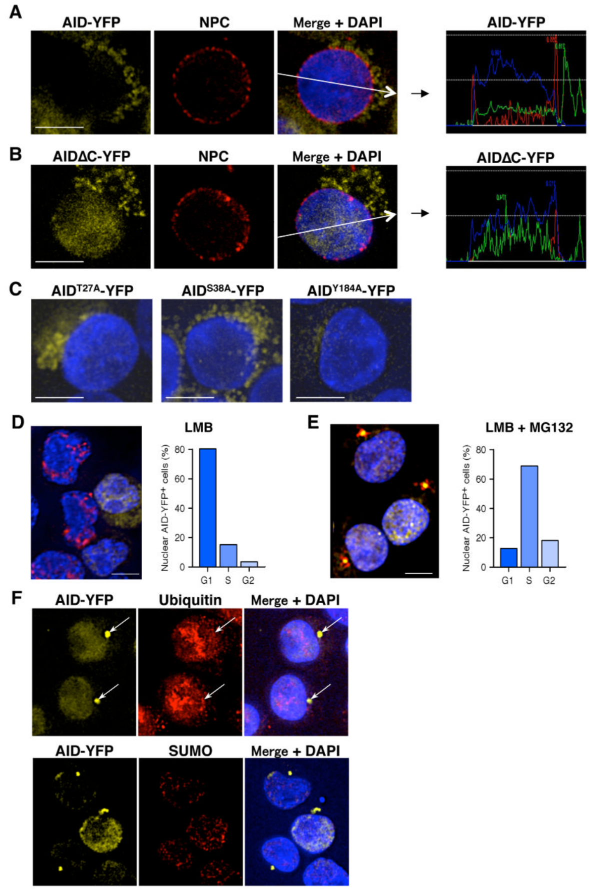

Figure 1.

Regulated nuclear localization of AID.

(*A*) AID-YFP predominantly localizes to the cytoplasm. *Left*, Representative images of DT40 AID-YFP stable transfectants. Nuclear pore complex (NPC) stained with antibodies (red, center), and merged DAPI image (right). Bar, 5 μm. *Right*, Subcellular distribution of AID-YFP analyzed with a line profile tool of the softWoRx imaging software.

(*B*) AIDΔC-YFP predominantly localizes to the nucleus. Notations as in panel A.

(*C*) Phosphorylation may regulate AID-YFP localization. Representative merged DAPI images of DT40 AID^{T27A}-YFP, AID^{S38A}-YFP and AID^{Y184A}-YFP stable transfectants.

(*D*) AID-YFP is present in the nucleus in G1 phase. *Left*, Representative images of DT40 AID-YFP cells treated with LMB (50 ng/ml, 1 hr), then labeled with BrdU (10 μM, 30 min). Bar, 5 μm. *Right*, Cell cycle distribution of cells containing nuclear AID-YFP (21%; n = 123 cells), as determined by BrdU staining and nuclear size.

(*E*) AID-YFP may be degraded in the nucleus in S phase. *Left*, Representative images of DT40 AID-YFP cells treated with MG132 (50 μM, 4 hr) and LMB (50 ng/ml, 1 hr); Golgi apparatus stained with antibodies (red). Bar, 5 μm. *Right*, Cell cycle distribution of DT40 AID-YFP cells treated with MG132 and LMB, which contain nuclear AID-YFP (18%; n = 298 cells).

(*F*) AID-YFP may form aggresomes following MG132 treatment. Representative images of DT40 AID-YFP cells treated with MG132 (50 μM, 4 hr) and LMB (50 ng/ml, 1 hr), and stained with antibodies to ubiquitin or SUMO (red, center); and merged DAPI image (right). Arrows indicate potential colocalization of AID-YFP and ubiquitin staining signal.

NIH-PA Author Manuscript
NIH-PA Author Manuscript

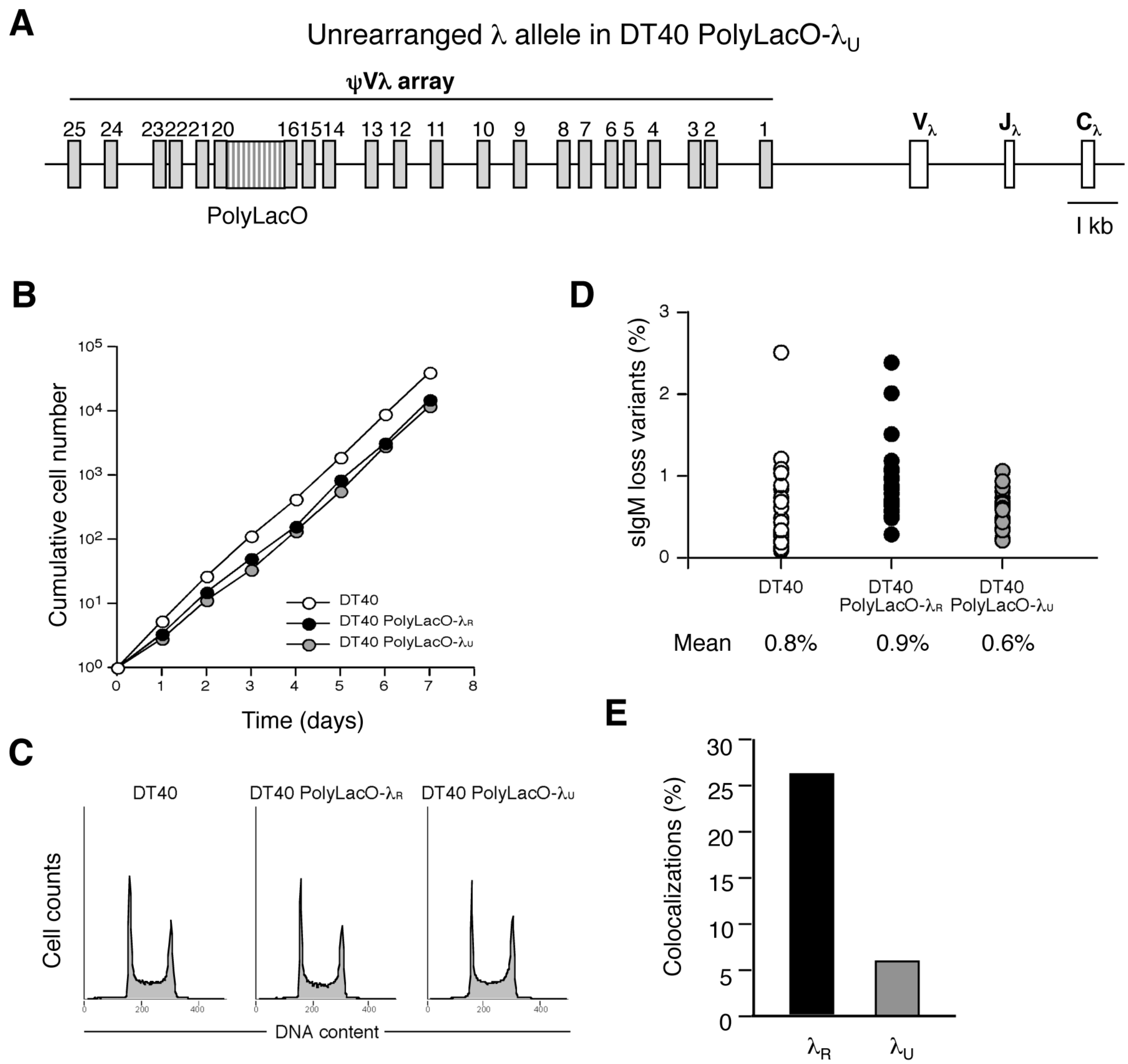

Figure 2.

E2A preferentially colocalizes with the rearranged λ_R allele.

(*A*) Schematic of the PolyLacO-tagged unrearranged Igλ locus in DT40 PolyLacO-λ_U cells. The ψVλ array, variable (V_λ), joining (J_λ), and constant (C_λ) regions are shown. PolyLacO is integrated between ψV17 and ψV20.

(*B*) Proliferation of DT40, DT40 PolyLacO-λ_R and DT40 PolyLacO-λ_U cells. Cell counting and culture passage were carried out daily and growth rate was calculated as a cumulative cell number. Data shown are the average from two separate experiments.

(*C*) Cell cycle profile of DT40, DT40 PolyLacO-λ_R and DT40 PolyLacO-λ_U cells. Exponentially growing cells were analyzed by flow cytometry after staining with propidium iodide.

(*D*) Accumulation of sIgM-loss variants by DT40, DT40 PolyLacO-λ_R and DT40 PolyLacO-λ_U cells. Frequencies of sIgM-loss variants in 24 subclones from each line were quantitated by flow cytometry following 6 weeks of clonal expansion. Mean sIgM-loss frequencies were 0.8%, 0.9% and 0.6%, respectively, as indicated at the bottom of the panel.

(*E*) Comparison of levels of colocalizations of E2A with the rearranged λ_R allele in DT40 PolyLacO-λ_R cells or the unrearranged λ_U allele in DT40 PolyLacO-λ_U cells.

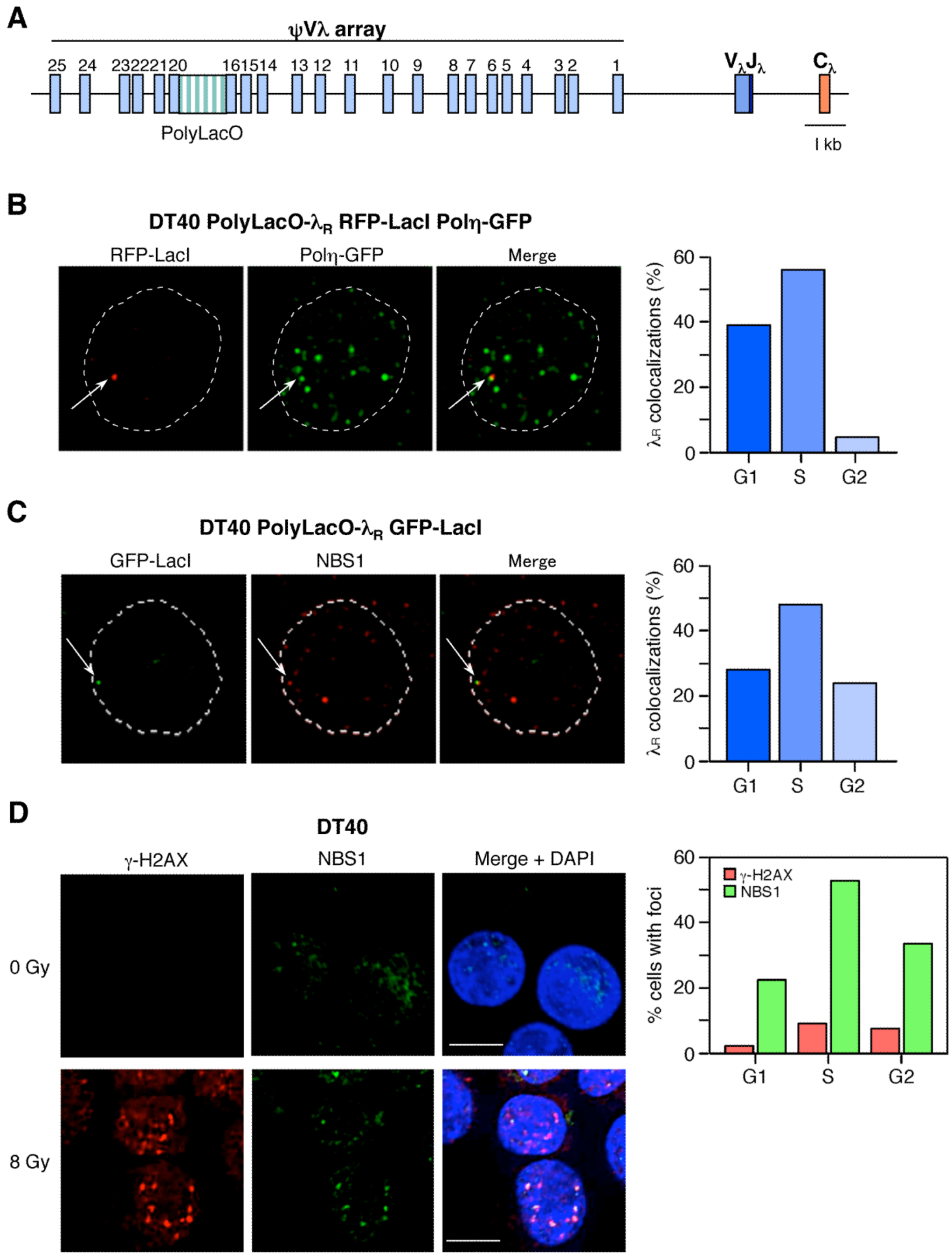

Figure 3.

Colocalizations of rearranged λ_R genes with Polη and MRN.

(*A*) Schematic of the PolyLacO-tagged rearranged Igλ locus in DT40 PolyLacO-λ_R cells. The upstream ψVλ array, variable (V_λ), joining (J_λ), and constant (C_λ) regions are shown. PolyLacO is integrated between ψV17 and ψV20.

(*B*) *Left*, Representative image of λ_R/Polη-GFP colocalization in DT40 PolyLacO-λ_R RFP-LacI Polη-GFP cells. Nuclear perimeter as determined by DAPI staining is outlined by the dashed white line; arrows point to colocalizations. Colocalizations were observed in 11% of cells (n = 1013), in two experiments. *Right*, Cell cycle distribution of total λ_R/Polη-GFP colocalizations; cell cycle was determined by analysis of nuclear radius (n = 79).

(*C*) *Left*, Representative image of λ_R/NBS1 colocalization in DT40 PolyLacO-λ_R GFP-LacI cells. Notations as in *B*. Colocalizations were observed in 17% of cells (*n* = 232 cells), in two experiments). *Right*, Cell cycle distribution of total λ_R/NBS1 colocalizations; cell cycle was determined by analysis of nuclear radius (*n* = 75).

(*D*) *Above left*, Representative immunofluorescent images of DT40, unirradiated (0 Gy), stained with anti-γ-H2AX (left) and anti-NBS1 (center) antibodies; merged DAPI image (right); bar, 10 μm. *Above right*, Percent of cells containing γ-H2AX or NBS1 foci in each stage of cell cycle; no colocalization; *n* = 410 cells; three experiments. *Below*, Representative immunofluorescent images of DT40, irradiated (8 Gy, 2 hrs post IR) and stained as above; 38% colocalization; *n* = 312 cells; three experiments.

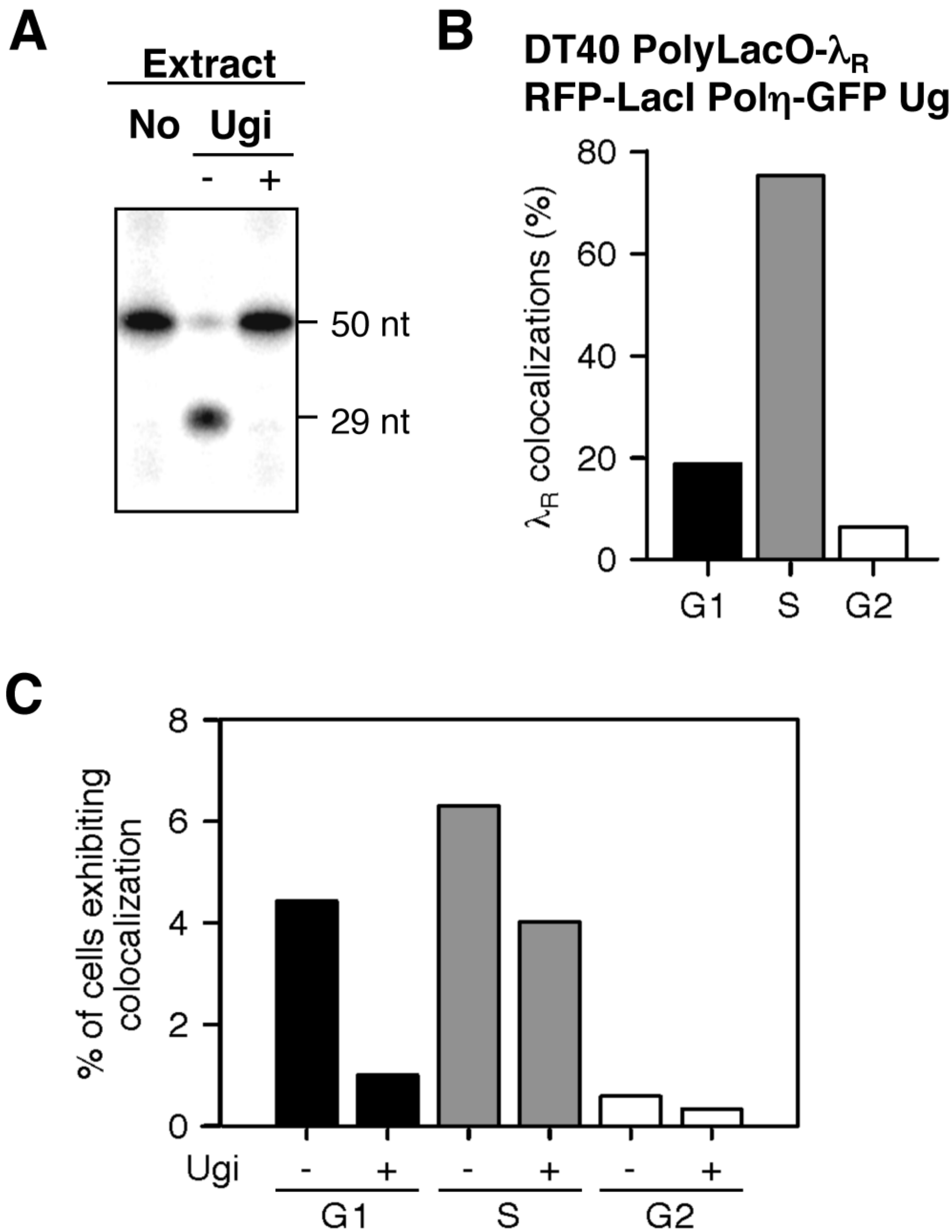

Figure 4.

UNG-dependent localizations of Polη-GFP at rearranged λ_R genes.

(*A*) Uracil-DNA excision activity in the nuclear extract of DT40 PolyLacO-λ_R RFP-LacI Polη-GFP cells or its derivative stably expressing Ugi (Ugi − and +, respectively).

(*B*) Cell cycle distribution of λ_R/Polη-GFP colocalizations in DT40 PolyLacO-λ_R RFP-LacI Polη-GFP Ugi cells (n = 16); 298 cells analyzed.

(*C*) Fraction of λ_R/Polη-GFP colocalizations in each stage of cell cycle, presented as the percent of total cells in which colocalizations were evident. Ugi expression diminished total colocalizations by about one-half.

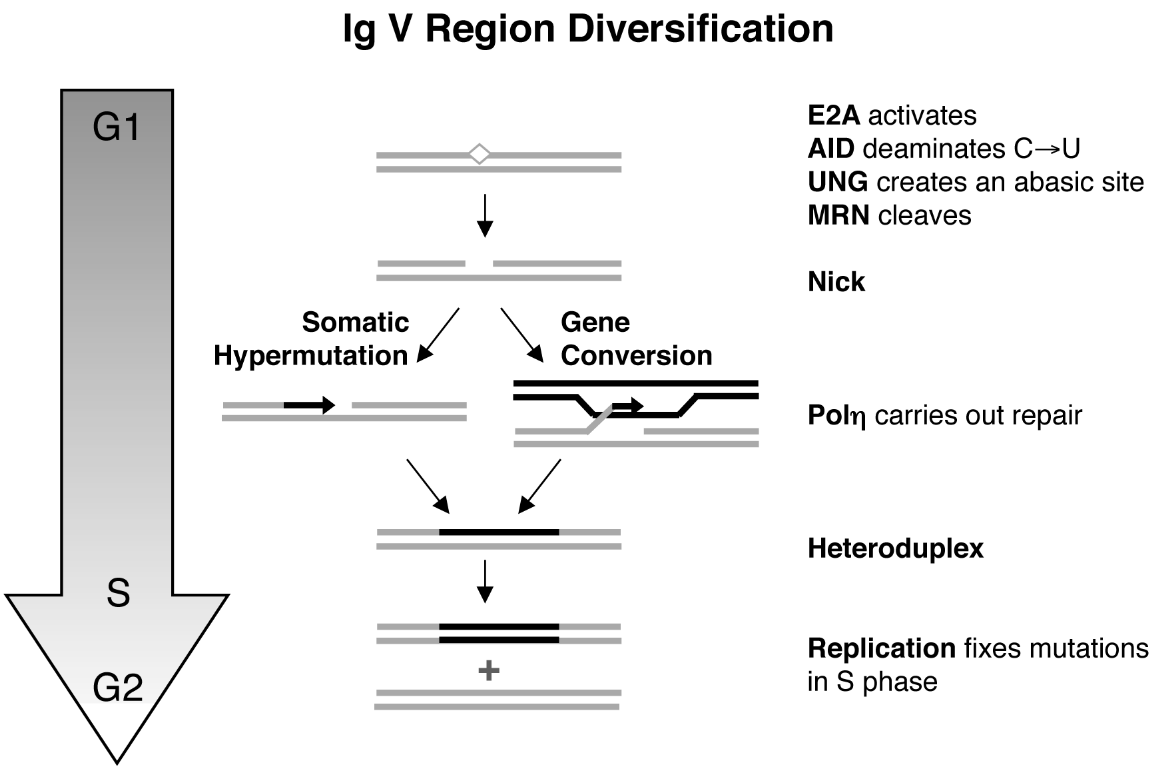

Figure 5.
Model for temporal regulation of Ig V region diversification.
Diversification is activated by E2A, initiated by DNA deamination by AID and deglycosylation by UNG, generating an AP site (diamond) which is cleaved by MRN, creating a nick. The nick primes nontemplated (somatic hypermutation, left), or templated (gene conversion, right) repair DNA synthesis by Polη. Ig V region diversification may be initiated and nearly completed in G1 phase of cell cycle, producing a heteroduplex. Replication in S phase fixes mutations. If initial mutagenesis affects only a single DNA strand, then one mutated and one germline chromatid will segregate in G2 phase.

Table I

Nuclear AID-YFP is absent from S phase cells

First treatment [a]	Second treatment [b]	BrdU+ [c]	nuclear AID-YFP+ [d]	nuclear AID-YFP+ and BrdU+ [c,d]	number of cells
LMB	LMB & BrdU	36%	19%	2.4%	288
BrdU	BrdU & LMB	32%	12%	1.1%	353

[a] Cells were first treated with LMB (50 ng/ml) or BrdU (10 μM), as indicated, for 30 min (t = 0 to 30 min).

[b] Incubation was continued with both compounds, as indicated, for 30 min (t = 30 to 60 min).

[c] Percentage of cells containing five or more distinct BrdU foci were scored as BrdU+.

[d] Nuclear localization of AID-YFP was examined using a line profile tool of the softWoRx software (Applied Precision), and cells scored as positive if a YFP signal above background was detected throughout the nucleus.